3D Modeling of the Relievo Based on the Computer Active Vision

Gui Wu[1, a], Jun Tao [2.b, 3, c]

[1.]Educational Administration office, Jianghan University, Wuhan 430056

[2.]School of Mathematics and Computer Science, Jianghan University, Wuhan 430056

[3.]Department of Electrical & Computer Engineering, Rowan University, Glassboro, New Jersey, USA 08028

[a]wugui214@163.com, [b]martintao2006@163.com, [c]taoj0@students.rowan.edu

Keywords: 3D Modeling; Small relieve; Calibration; Slide projector; Computer active vision; Photogrammetry

Abstract. At present, the 3D modeling of the small relievo which is lack of real texture or no real texture is a huge difficulty and challenge. The paper provides a good way based on the computer active vision. The slide projector as an active sensor is steered in the principle of the traditional binocular vision. The slide projector could supply the designed texture features to the small relieve, which is easy to be extracted out and matched well because they are clear and stable. The space forward intersection method can compute out the space coordinates of the texture features. The final 3D model is built by connecting the neighbor space points. The 3D modeling of the small relievo based on the computer active vision is proved to be effective and practical by the experimental data and results.

Introduction

With the development of the image processing and the computer vision, the 3D modeling of the small relievo becomes a research field of the heritage conservation and the artistic creation. The digitalization of the small relievo provides the convenience and the advantage of the design, the production, the creation and the protection of the relievo.

The digital 3D reconstruction is referred as the recovery from the two-dimensional digital images because the exact three-dimensional information is lost during the two-dimensional digital image formation. The three-dimensional information or the depth information should be extract from the two-dimensional digital images. The matching of the corresponding points in the digital images is the key of the traditional method. When there is no feature point or is lack of the feature points on the targets, or when the corresponding points cannot be matched correctly, the 3D modeling would become difficult and hard.

The surface of the small relievo is always glossy and sequent so that it is difficult to find texture feature which is the key point of the digital 3D modeling. The computer active vision could help to resolve this problem effectively. A slide projector as the active sensor is steered into the equipment system. The slide projector can design and generate the structure illumination on the original images. The 3D modeling of the small relievo is entirely based on the strict theory of the binocular vision. The 3D modeling method provided by the paper is untouched so that it is nondestructive which is just suitable for the protection and preservation of the small relievo.

Calibration of the Slide Projector and the Digital Camera

The Digital Camera Calibration. The digital camera calibration is an important step at first, because its intrinsic and extrinsic parameters are used to compute the coordinates of the space feature points. And these parameters are the basic data for the calibration of the slide projector in the next step.

The collinear equations are:

$$x - x_0 = -f \frac{a_1(X-X_s)+b_1(Y-Y_s)+c_1(Z-Z_s)}{a_3(X-X_s)+b_3(Y-Y_s)+c_3(Z-Z_s)}$$

$$y - y_0 = -f \frac{a_2(X-X_s)+b_2(Y-Y_s)+c_2(Z-Z_s)}{a_3(X-X_s)+b_3(Y-Y_s)+c_3(Z-Z_s)}$$

(1)

Where, f, x0, y0 are the intrinsic parameters of the digital camera, Xs, Ys, Zs are the coordinates of the digital camera center, X, Y, Z are the space coordinates of points and x, y are the image coordinates of the relative points. R={ai, bi, ci, i=1,2,3} is the rotated matrix made up of rotated angles ϕ, ω, κ. The coordinates of Z of the points are zero.

$$x = \frac{\left(f\frac{a_1}{\lambda} - \frac{a_3}{\lambda}x_0\right)X + \left(f\frac{b_1}{\lambda} - \frac{b_3}{\lambda}x_0\right)Y + \left(x_0 - \frac{f}{\lambda}(a_1X_s + b_1Y_s + c_1Z_s)\right)}{-\frac{a_3}{\lambda}X - \frac{b_3}{\lambda}Y + 1}$$

$$y = \frac{\left(f\frac{a_2}{\lambda} - \frac{a_3}{\lambda}y_0\right)X + \left(f\frac{b_2}{\lambda} - \frac{b_3}{\lambda}y_0\right)Y + \left(y_0 - \frac{f}{\lambda}(a_2X_s + b_2Y_s + c_2Z_s)\right)}{-\frac{a_3}{\lambda}X - \frac{b_3}{\lambda}Y + 1}$$

(2)

Where $\lambda = (a_3X_s + b_3Y_s + c_3Z_s)$.

$$\begin{cases} h_1 = f\frac{a_1}{\lambda} - \frac{a_3}{\lambda}x_0 \\ h_2 = f\frac{b_1}{\lambda} - \frac{b_3}{\lambda}x_0 \end{cases}, \begin{cases} h_4 = f\frac{a_2}{\lambda} - \frac{a_3}{\lambda}y_0 \\ h_5 = f\frac{b_2}{\lambda} - \frac{b_3}{\lambda}y_0 \end{cases}, \begin{cases} h_3 = x_0 - \frac{f}{\lambda}(a_1X_s + b_1Y_s + c_1Z_s) \\ h_6 = y_0 - \frac{f}{\lambda}(a_2X_s + b_2Y_s + c_2Z_s) \end{cases}, \begin{cases} h_7 = -\frac{a_3}{\lambda} \\ h_8 = -\frac{b_3}{\lambda} \end{cases}$$

(3)

Changing formula (3) to reduce the parameter λ, and $a_1b_1 + a_2b_2 + a_3b_3 = 0$, then:

$$f = \sqrt{\frac{-(h_1 - h_7x_0)\cdot(h_2 - h_8x_0) - (h_4 - h_7y_0)\cdot(h_5 - h_8y_0)}{h_7h_8}}$$

(4)

If the digital camera is not a common one but a special measuring camera, the calibration would be cancelled because its intrinsic parameters are the known data already. However, its extrinsic parameters are still required to be calculated out first.

The Slide Projector Calibration. Using the same calibration algorithm of the digital camera, the slide projector is also calibrated completely and successful by using the intrinsic and the extrinsic parameters of the calibration data of the digital camera. The calibration key is also same to compute the coordinates of the space points and the image points.

The camera position needs to be fixed after it is calibrated completely so that its parameters could be used for the calibration of the slide projector. The image points of the slide projector calibration are designed in the slide with the same shape of the digital camera calibration. The space points of the slide projector calibration are calculated out by the images of the digital camera calibration.

By the collinear equations and the image processing method, the decomposition of the initial values of the intrinsic and the extrinsic parameters is deduced. By the platform rotating continually, the sequence of images are taken from the different orientations. All images need to be from two different orientations at least. So there are two sets of the initial values of the parameters of the slide projector.

The intrinsic parameters of the slide projector could be computed out by the whole adjustment based on these initial values. Thence, the slide projector calibration is finished entirely by the way.

Equipments and Methodology

At present, most computer vision systems still use a static camera. However, the slide projector as an active sensor is steered into the whole equipment system based on the computer active vision. The slide projector in place of a digital camera supplies the convenience and the flexibility to the 3D modeling in the principle of the binocular vision.

The slide of the projector is easy to be designed as the image factor which makes the whole system become active and flexible. In addition of the small relievo lack of the texture features, the slide projector could supply the manual feature onto the surface of the small relievo which makes its 3D modeling practically and applicably.

After the calibration of the slide projector and the digital camera in advance, the whole system is similar with the binocular vision system in the principle of 3D modeling.

The Equipment System. The equipment system is composed of the digital camera, the slide projector, the control platform and the computer. The computer controls the other three devices automatically working together. The control platform is a rotating plane whose function is for the calibration of the projector and the camera. The digital camera function is to take images as the original data. The slide projector could provide the active source for the target and work instead of a digital camera at the same time.

The entire system is easy to get relatively and setup to be connected with each other. The system could settle down conveniently in a room with the enough lights. The diagram of the system is shown on the Fig. 1 as following.
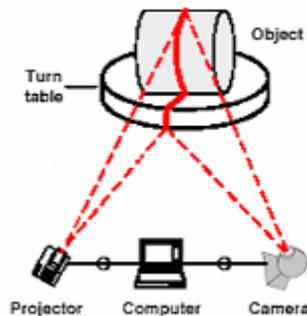

Figure 1. The principle of whole equipments

Algorithm of the Method. Based on the collinear equations shown on the formula 1 above, four equations is listed ordinarily according to a pair of the homologous points. The space coordinates only need three equations for the calculation. By the line matching shown on the Fig. 2, there exist three known equations already.

Figure 2. The line matching

From the formula 1, there are x = xr, y = yr, then:

$$[a_3+f_r\frac{a_1}{(x_r-x_{r0})}]X+[b_3+f_r\frac{b_1}{(x_r-x_{r0})}]Y+[c_3+f_r\frac{c_1}{(x_r-x_{r0})}]Z=$$

$$[a_3+f_r\frac{a_1}{(x_r-x_{r0})}]X_{rs}+[b_3+f_r\frac{b_1}{(x_r-x_{r0})}]Y_{rs}+[c_3+f_r\frac{c_1}{(x_r-x_{r0})}]Z_{rs}$$

$$[a_3+f_r\frac{a_2}{(y_r-y_{r0})}]X+[b_3+f_r\frac{b_2}{(y_r-y_{r0})}]Y+[c_3+f_r\frac{c_2}{(y_r-y_{r0})}]Z=$$

$$[a_3+f_r\frac{a_2}{(y_r-y_{r0})}]X_{rs}+[b_3+f_r\frac{b_2}{(y_r-y_{r0})}]Y_{rs}+[c_3+f_r\frac{c_2}{(y_r-y_{r0})}]Z_{rs}$$

There is a corresponding line in the projected slide according to the point on the curve of the image taken by the digital camera and its equation is x = xl. From the formula 1, then:

$$[a_6+f_l\frac{a_4}{(x_l-x_{l0})}]X+[b_6+f_l\frac{b_4}{(x_l-x_{l0})}]Y+[c_6+f_l\frac{c_4}{(x_l-x_{l0})}]Z=$$

$$[a_6+f_l\frac{a_4}{(x_l-x_{l0})}]X_{ls}+[b_6+f_l\frac{b_4}{(x_l-x_{l0})}]Y_{ls}+[c_6+f_l\frac{c_4}{(x_l-x_{l0})}]Z_{ls}$$

From the two formulas above, then:

$$X=\frac{\begin{vmatrix}[a_3+f_r\frac{a_1}{(x_r-x_{r0})}]X_{rs}+[b_3+f_r\frac{b_1}{(x_r-x_{r0})}]Y_{rs}+[c_3+f_r\frac{c_1}{(x_r-x_{r0})}]Z_{rs} & [b_3+f_r\frac{b_1}{(x_r-x_{r0})}] & [c_3+f_r\frac{c_1}{(x_r-x_{r0})}] \\ [a_3+f_r\frac{a_2}{(y_r-y_{r0})}]X_{rs}+[b_3+f_r\frac{b_2}{(y_r-y_{r0})}]Y_{rs}+[c_3+f_r\frac{c_2}{(y_r-y_{r0})}]Z_{rs} & [b_3+f_r\frac{b_2}{(y_r-y_{r0})}] & [c_3+f_r\frac{c_2}{(y_r-y_{r0})}] \\ [a_6+f_l\frac{a_4}{(x_l-x_{l0})}]X_{ls}+[b_6+f_l\frac{b_4}{(x_l-x_{l0})}]Y_{ls}+[c_6+f_l\frac{c_4}{(x_l-x_{l0})}]Z_{ls} & [b_6+f_l\frac{b_4}{(x_l-x_{l0})}] & [c_6+f_l\frac{c_4}{(x_l-x_{l0})}]\end{vmatrix}}{\Delta}$$

$$Y=\frac{\begin{vmatrix}[a_3+f_r\frac{a_1}{(x_r-x_{r0})}] & [a_3+f_r\frac{a_1}{(x_r-x_{r0})}]X_{rs}+[b_3+f_r\frac{b_1}{(x_r-x_{r0})}]Y_{rs}+[c_3+f_r\frac{c_1}{(x_r-x_{r0})}]Z_{rs} & [c_3+f_r\frac{c_1}{(x_r-x_{r0})}] \\ [a_3+f_r\frac{a_2}{(y_r-y_{r0})}] & [a_3+f_r\frac{a_2}{(y_r-y_{r0})}]X_{rs}+[b_3+f_r\frac{b_2}{(y_r-y_{r0})}]Y_{rs}+[c_3+f_r\frac{c_2}{(y_r-y_{r0})}]Z_{rs} & [c_3+f_r\frac{c_2}{(y_r-y_{r0})}] \\ [a_6+f_l\frac{a_4}{(x_l-x_{l0})}] & [a_6+f_l\frac{a_4}{(x_l-x_{l0})}]X_{ls}+[b_6+f_l\frac{b_4}{(x_l-x_{l0})}]Y_{ls}+[c_6+f_l\frac{c_4}{(x_l-x_{l0})}]Z_{ls} & [c_6+f_l\frac{c_4}{(x_l-x_{l0})}]\end{vmatrix}}{\Delta}$$

$$Z=\frac{\begin{vmatrix}[a_3+f_r\frac{a_1}{(x_r-x_{r0})}] & [b_3+f_r\frac{b_1}{(x_r-x_{r0})}] & [a_3+f_r\frac{a_1}{(x_r-x_{r0})}]X_{rs}+[b_3+f_r\frac{b_1}{(x_r-x_{r0})}]Y_{rs}+[c_3+f_r\frac{c_1}{(x_r-x_{r0})}]Z_{rs} \\ [a_3+f_r\frac{a_2}{(y_r-y_{r0})}] & [b_3+f_r\frac{b_2}{(y_r-y_{r0})}] & [a_3+f_r\frac{a_2}{(y_r-y_{r0})}]X_{rs}+[b_3+f_r\frac{b_2}{(y_r-y_{r0})}]Y_{rs}+[c_3+f_r\frac{c_2}{(y_r-y_{r0})}]Z_{rs} \\ [a_6+f_l\frac{a_4}{(x_l-x_{l0})}] & [b_6+f_l\frac{b_4}{(x_l-x_{l0})}] & [a_6+f_l\frac{a_4}{(x_l-x_{l0})}]X_{ls}+[b_6+f_l\frac{b_4}{(x_l-x_{l0})}]Y_{ls}+[c_6+f_l\frac{c_4}{(x_l-x_{l0})}]Z_{ls}\end{vmatrix}}{\Delta}$$

Where:

$$\Delta=\begin{vmatrix}[a_3+f_r\frac{a_1}{(x_r-x_{r0})}] & [b_3+f_r\frac{b_1}{(x_r-x_{r0})}] & [c_3+f_r\frac{c_1}{(x_r-x_{r0})}] \\ [a_3+f_r\frac{a_2}{(y_r-y_{r0})}] & [b_3+f_r\frac{b_2}{(y_r-y_{r0})}] & [c_3+f_r\frac{c_2}{(y_r-y_{r0})}] \\ [a_6+f_l\frac{a_4}{(x_l-x_{l0})}] & [b_6+f_l\frac{b_4}{(x_l-x_{l0})}] & [c_6+f_l\frac{c_4}{(x_l-x_{l0})}]\end{vmatrix}$$

At present, the space coordinates have been worked out.

Experiments and Results

According to the theory and the method described above, a couple of experiments are designed to test and check the data. The calibration and the 3D modeling use the same control platform. The target object is a small relievo because of the limitation of the size of the control platform.

The Calibration of the Projector and the Camera. The 60cm×60cm is the size of the control platform and there are 324 points in total. The interval of the points is the same 30mm. The size of the slide is designed as 1024 pixels×768 pixels and there are also 324 points in the slide. The interval of the points is the same 40 pixels.

The slide projector and the digital camera are fixed and focused respectively. There are four sets of the double images shown on the Fig. 3. The size of the each image is 1300pixels×1030pixels.
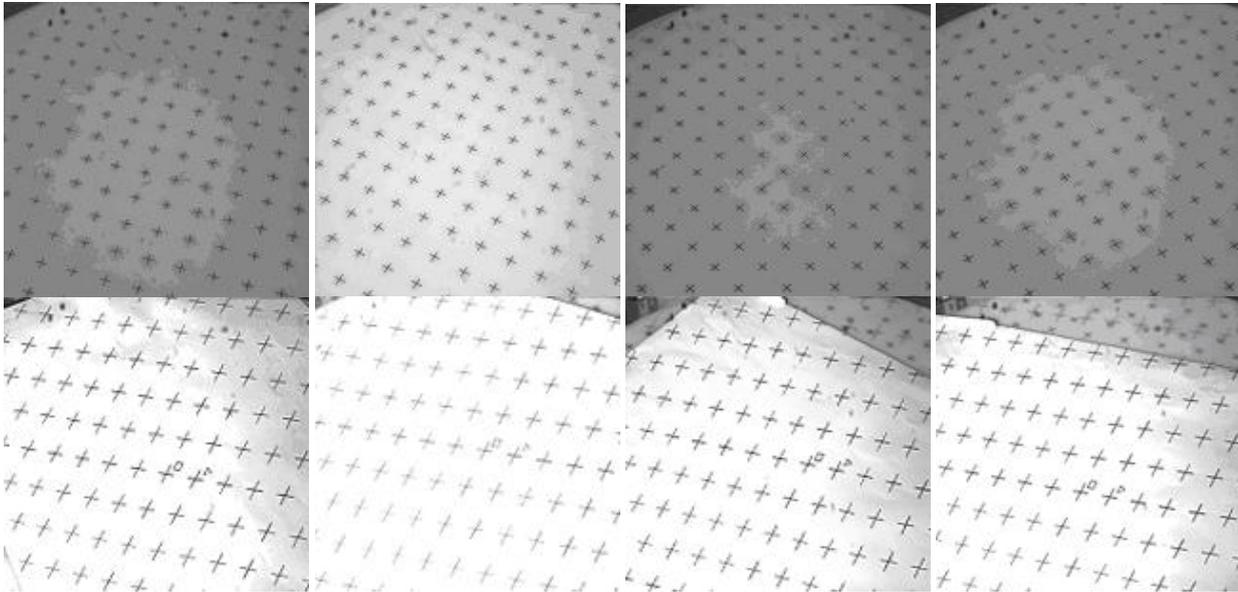
Figure 3. The original image data

By using these points on the image data, the experiment could calibrate the digital camera and the slide projector correctly and also compute the extrinsic parameters of both out entirely and correctly.

The parameters of the digital camera and the slide projector are shown on the Table 1 as following.

Table.1 The parameters

	Digital Camera	Slide Projector
f/pixel	3723.227916	1852.251838
x0/ pixel	647.158720	552.627441
y0/ pixel	516.352984	433.974580
Xs/mm	92.336316	-345.023227
Ys/mm	-837.369195	-862.925760
Zs/mm	616.363872	732.102576
Ψ/radian	-0.114012	0.454501
Ω/ radian	0.935347	0.832487
K/ radian	0.152368	-0.394113

3D Modeling of the Small Relievo. The small relievo is put on the center of the control platform. The slide projector projects the stripe from the slide onto the surface of the small relievo. The size of the slide is designed as 1024 pixels×768 pixels. The manual feature is designed as stripe which is clear to show on the surface and is better to be matched in the images.

One of the original images is shown on the Fig. 4 as following.
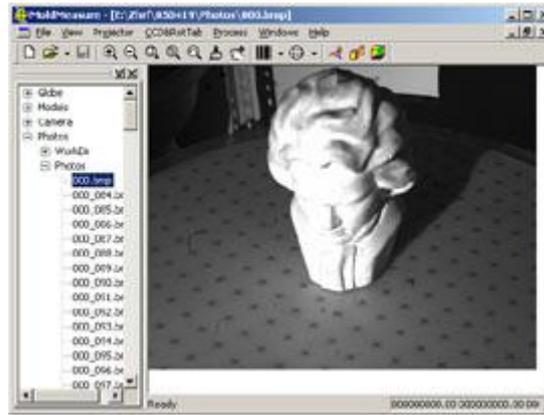
Figure 4. The original image data

Using the method provided by the paper to process the original image data, the point cloud of the space feature points of the small relievo is gained and shown on the Fig. 5 as following.
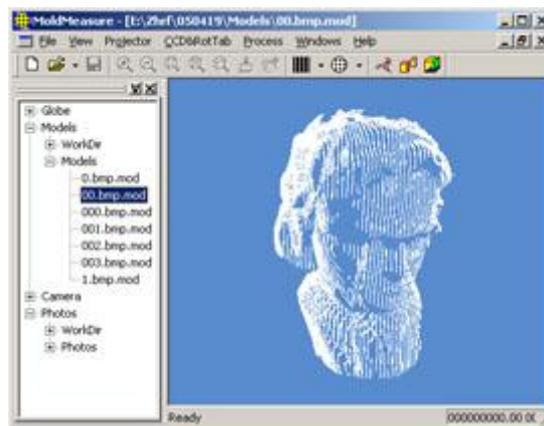

Figure 5. The space point cloud

According to the method above, all points projected on the surface of the small relievo could be connected together. The 3D modeling of the small relievo is completed successfully.

Conclusion

The 3D modeling of the small   elieve proposed in the paper is confirmed to be correct and effective by the experimental data and results. The 3D modeling method is active and effective because the active sensor is introduced into the system and the projected feature could be designed first on motivation.

The 3D modeling method is non-touched so that it is remote and nondestructive. Because of the little effect by the space factor or the time factor, the 3D modeling of the small   elieve based on the computer active vision is flexible and practical.

References

[1] Guiying Li, B. Junlong Liu, Chunhui Jiang, and Ke Tang, "Relief Impression Imamge Detection: Unsupervised Extracting Objrects Directly From Feature Arrangements," Phil. Trans. Roy. Soc. London, vol. A247, pp. 529-551, January 2016.

[2] Russakovsky, J. Deng, H. Su, J. Krause, S. Satheesh, Z. Huang, et al, "Image large scale visual recognition challenge," International Journal of Computer Vision, 2014, pp.1-42.

[3] R. Girshick, J. Donahue, T. Darrell, and J. Malik, "Rich feature hierarchies ofr accurate object detection and semantic segmentation," in Computer Vision and Pattern Recognition,, 2014, pp. 580-587.

[4] J. R. Uijlings, K. E. van de Sande, T. Gevers, and A. W. smeulders, "Selective search for object recognition," International journal of computer vision, vol. 104, no. 2, pp. 154-171, 2013.

[5] H. O. Song, R. Girshick, S. Jegelka, J. Mairal, Z. Harchaoui, and T. Darrell, "On learning to localize objects with minimal supervision,"in Processing of the International Conference on Machine Learning, 2014.

[6] Y. Yorozu, M. Hirano, K. Oka, and Y. Tagawa, "Binarized normed gradients for objectness estimation," in Computer Visiion and Pattern Recognition, 2014, pp. 3286-3293.

[7] A. Ghodrati, A. Diba, M. Pedersoli, T. Tuytelaars, and L. Van Gool, "Hunting objects by cascading deep convolutional layers," in Processing of the IEEE International Conference on Computer Vision, 2015, pp, 2578-2586.

[8] C. –W. Chou, O. Teytaud, S. –J. Yen, "Active object localization with deep reinforcement learning," Volume 6624 of the series Lecture Notes in Computer Science pp 3273-3282, 2011.

[9] Yuxia Sun, Shenyang, China, Cheng Liu, Hongkun Qiu, "Delving deep into rectifiers surpassing human level performance on imagenet classification," in Computer Visiion and Pattern Recognition, pp. 1178 − 1182, 2013.

[10] Jun Tao, "3D modeling of small object based on the projector-camera system," in Kybernetes, Vol.41, No.9, 1269-1276, 2012.

[11] Yen Shi-Jim, Yang Jung-Kuei, "A trainable system for object detection." International Journal of Computer Vision, Vol.3, No.2, 100-118, 2011.

[12] Sharma, S., Kobti, Z., Goodwin, S., "Knowledge generation for improving simulations in UCT for general game playing," In: Wobcke, W., Zhang, M. (eds.) AI 2008. LNCS (LNAI), vol. 5360, pp. 49–55. Springer, Heidelberg, 2012.

[13] Jun Tao, "Development and application of functionally gradient materials," in Processing of International conference on industrial control and electronics engineering, 1022-1025, 2012.

[14] Qiao Zhihua, Yang Ming, Wang Zijuan, "Visualizing and understanding convolutional networks," in Computer Vision- ECCV, pp. 679-682, 2014.

[15] Rolet, P., Sebag, M., Teytaud, O., "Integrated recognition, localization and detection using convolutional networks," In: Proceedings of the ECML Conference, pp. 1255-1263, 2012.

[16] Jun Tao, "Design and visualization of optical feedback laser based on computer vision," in Processing of International conference on industrial control and electronics engineering, 1030-1032, 2012.

[17] De Mesmay, F., Rimmel, A., Voronenko, Y., Püschel, M., "Convolutional feature masking for joint object and stuff segmentation," In ACM International Conference Proceeding Series, vol. 382, p. 92. ACM, New York, 2013.

[18] Lee, C.-S., Wang, M.-H., Chaslot, G., Hoock, J.-B., Rimmel, A., Teytaud, O., Tsai, S.-R., Hsu, S.-C., Hong, T.-P., "The pascal visual object classes challenge: A retrospective," International Journal of Computer Vision, vol. 111, no. 1, pp, 98-136, 2014.

[19] Jun Tao, "Face reconstruction based on camera-projector system," in Processing of International conference on industrial control and electronics engineering, 1026-1029, 2012.

[20] Chaslot, G., Winands, M., Uiterwijk, J., van den Herik, H., Bouzy, B., "Progressive Strategies for Monte-Carlo Tree Search," In Proceedings of the 10th Joint Conference on Information Sciences (JCIS 2007), pp. 655–661. World Scientific Publishing Co. Pte. Ltd., Singapore, 2013.

[21] Auer, P., "Using confidence bounds for exploitation-exploration trade-offs," in The Journal of Machine Learning Research 3, 397–422, 2013.

[22] Bourki, A., Chaslot, G., Coulm, M., Danjean, V., Doghmen, H., Hoock, J.-B., Hérault, T., Rimmel, A., Teytaud, F., Teytaud, O., Vayssière, P., Yu, Z., "Scalability and parallelization of monte-carlo tree search," In Proceedings of Advances in Computer Games 13, 2010.